Cascading failures in networks of heterogeneous node behavior

O. Smith,[1,*] J. Crowe,[2] E. Farcot,[1] R. D. O'Dea,[1] and K. I. Hopcraft[1]

[1]*School of Mathematical Sciences, University of Nottingham, Nottingham NG7 2RD, United Kingdom*
[2]*Faculty of Engineering, University of Nottingham, Nottingham NG7 2RD, United Kingdom*

Variability in the dynamical function of nodes comprising a complex network impacts upon cascading failures that can compromise the network's ability to operate. Node types correspond to sources, sinks, or passive conduits of a current flow, applicable to renewable electrical power microgrids containing a variable number of intermittently operating generators and consumers of power. The resilience to cascading failures of ensembles of synthetic networks with different topology is examined as a function of the edge current carrying capacity and mix of node types, together with exemplar real-world networks. While a network with a homogeneous composition of node types can be resilient to failure, one with an identical topology but with heterogeneous nodes can be strongly susceptible to failure. For networks with similar numbers of sources, sinks, and passive nodes the mean resilience decreases as networks become more disordered. Nevertheless all network topologies have enhanced regions of resilience, accessible by the manipulation of node composition and functionality.

Naturally occurring examples of complex networks include, *inter alia*, transportation, economic, and social structures, biological systems, and power grids. When a dynamic is imposed upon these structures, their ability to operate can be compromised by a part of the network, be it an edge or node, developing a fault which then spreads in a cascade throughout the entirety [1,2]. Catastrophic events such as blackouts in electrical grids [3], crashes in financial markets [4,5], and the spread of congestion and overloads in the Internet and transportation networks [6], can be described as cascading failures. A threshold cascade model was introduced in Ref. [7], in which a node in a network fails with probability proportional to the number of adjacent failed nodes. It showed that networks with heterogeneous degree distributions have increased resilience. A flow-based cascade model, applied to large-scale electrical grids and the Internet, was studied in Refs. [8,9] and highlighted the vulnerability of networks whose nodes possess heterogeneous capacities and bear a load proportional to their degree. Selective pruning of a network topology was shown to help arrest cascades in Refs. [10,11], while a rewiring scheme to suppress cascades was considered in Ref. [12]. Cascades have been studied on large-scale power grid topologies in Ref. [13], and in Ref. [14] which showed that large-scale cascades are most likely to be triggered by edges in the vicinity of a network's core. Cascades have also been investigated using a continuous-time model [15], oscillator networks [16,17], and in so-called interdependent or multiplex networks [18,19].

These studies consider networks with fixed node types and behavior; however, Ref. [20] showed that different node types affect network efficiency and redundancy, which is allied to resilience. This Rapid Communication will identify regimes of resilience to cascading failure in terms of such heterogeneity of node types, be they generators, consumers, or passive carriers of flow. This is motivated by the increasing proliferation of small renewable energy resources in modern electrical grids. Such microgrids possess a variable number of mutable consumers and generators of power that are typically spread throughout the networks, and these intermittent sources and sinks generally have small output and consumption. This contrasts with the rigid structure of traditional power grids which contain a small number of large-capacity generators. Understanding how this increased spread in location and variability in node function affects the operation, stability, and robustness of electrical networks is an important and ongoing interdisciplinary problem [21–24] that we address.

We consider networks $\mathcal{G} = (\mathcal{V}, \mathcal{E})$, with $n = |\mathcal{V}|$ nodes and $m = |\mathcal{E}|$ edges, wherein n_s nodes are sources of flow, n_d are sinks, and the remaining n_p are passive or empty. Each edge $e \in \mathcal{E}$ has a flow volume F_e, computed using the linearized dc power flow equation [25]

$$F_e = \langle E_e, \theta \rangle / x_e. \tag{1}$$

Here, x_e is the reactance of edge e and $E \in \mathbb{R}^{n \times m}$ is the node-edge incidence matrix, with E_e its eth column. The inner product is denoted by $\langle \cdot, \cdot \rangle$ and $\theta \in \mathbb{R}^n$ is the vector of node voltage phases determined from

$$\mathcal{L}\theta = P, \tag{2}$$

where $\mathcal{L} = E \operatorname{diag}(Y)E^T$ is the weighted graph Laplacian and $Y \in \mathbb{R}^m$ the vector with entries $1/x_e$. The flow injection vector $P \in \mathbb{R}^n$ has entries

$$P_v = \begin{cases} (1 + \zeta_v)P^{\mathrm{tot}}/n_s, & \text{if node } v \text{ is a source,} \\ -(1 + \zeta_v)P^{\mathrm{tot}}/n_d, & \text{if node } v \text{ is a sink,} \\ 0, & \text{otherwise,} \end{cases} \tag{3}$$
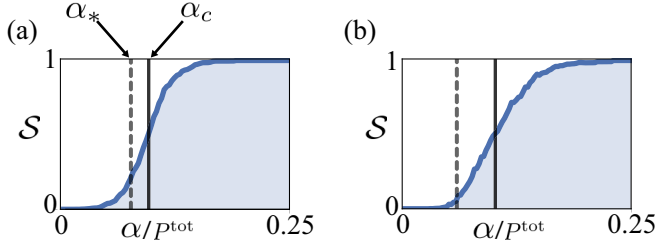
*oliver.smith@nottingham.ac.uk

FIG. 1. The mean fraction $\mathcal{S}$ of surviving edges as a function of edge capacity α for ensembles of 200 Watts-Strogatz networks with $n = 50$, $K = 4$, $n_s = 10$, and $n_d = 40$. (a) and (b) are for $q = 0.1$ and 1, respectively.

with P^{tot} the total power injected into the network and ζ_v a random variable used to induce heterogeneity in source and sink strength.

Solutions of Eqs. (1) and (2) describe a flow where supply and demand is matched, and this will be enforced throughout a cascading failure, which proceeds as follows. A maximum capacity α is assigned to each edge of the network and a cascade is initiated by computing the equilibrium flow from Eqs. (1) and (2) and removing the most heavily loaded edge, then recalculating the flow F_e on each edge in this modified network. If $F_e > \alpha$ on any edge, that edge is deemed overloaded and removed. This process continues until the network attains a final equilibrium with all edges carrying a flow $\leqslant \alpha$. During this cascade the network may fragment into separate connected components, and so the algorithm must be recursively applied for each new connected component in which conservation of flow must be ensured. Flow surplus or deficit is prevented by adjusting the source and sink strengths. We assume that sources and sinks alter their demand and supply reciprocally. If a component contains n_s' sources, n_d' sinks, and a flow supply surplus δ, then each source decreases its output by $\delta/2n_s'$ and each sink increases its demand by $\delta/2n_d'$. If the component contains either no sources or no sinks then the flow cannot be balanced and the entire component is removed. Balancing of power by nonreciprocal source/sink behavior is discussed later, together with other models for initiating the cascade.

The network eventually attains a final state, with the fraction of surviving edges relative to the original number denoted by $\mathcal{S}$. A value of $\mathcal{S} = 0$ indicates an entire network failure; $\mathcal{S} = 1$ denotes complete resilience. To assess the resilience of networks to failure, $\mathcal{S}$ is computed as a function of α, as displayed in Figs. 1(a) and 1(b) for an ensemble of 200 random networks generated by the Watts-Strogatz method [26]. These are of size $n = 50$, comprising $n_s = 10$ and $n_d = 40$ nodes, with locations chosen uniformly at random, and chosen rewiring parameters $q = 0.1$, 1 characteristic of small-world and Poisson networks, respectively. Both networks are susceptible to substantial disruption for capacities $\alpha \lesssim 0.06$ and are essentially robust for $\alpha \gtrsim 0.2$. Half of the network survives at the critical value α_c, for which $\mathcal{S}(\alpha_c) = 1/2$. The smaller α_c is, the more resilient the network will be to failure. Figure 1 shows that α_c increases as the networks become more Poissonian. To operate nontrivially the network must initially contain some nonzero capacity α_*, and this is defined
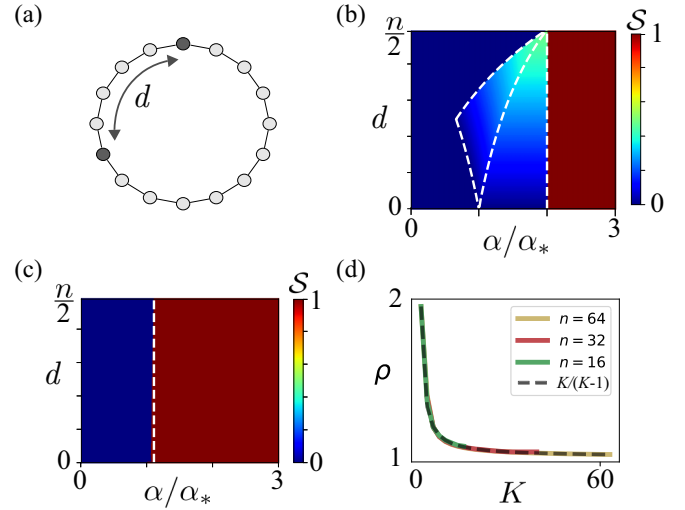

FIG. 2. (a) Periodic ring lattice with $K = 2$ containing $n_s = 2$ sources and $n_d = n - 2$ sinks with source separation d. (b) $\mathcal{S}(\alpha/\alpha_*, d)$ for $K = 2$. (c) $\mathcal{S}$ for $K = 10$. (d) $\rho(K)$ for periodic ring lattices of different sizes, with composition $n_s = 1$ and $n_d = n - 1$, showing the approximation $K/(K - 1)$.

from the initial flow configuration F_0 to be $\alpha_* = \max(F_0)$. The ensemble average values of α_* are also shown in Figs. 1(a) and 1(b).

The fraction of surviving edges $\mathcal{S}$ depends on network size, topology, and both composition and location of the node types. To gain insight into this dependence it is instructive to consider an exemplar network of n nodes with a simple ring structure, such as that illustrated in Fig. 2(a) that has $n_s = 2$, $n_d = n - 2$, common degree $K = 2$, and shortest path distance between the two sources d. The dependence of $\mathcal{S}$ on the configuration space of α/α_* and d is shown in Fig. 2(b), within which distinct regions with defined boundaries can be identified analytically [27], as overlaid in the figure. Crucially for $\alpha/\alpha_* \geqslant 2$, this network is resilient to cascading failures independent of the relative location of the sources, whereas for $\alpha/\alpha_* < 2$ the network is less robust with resilience conditional on the flow capacity and d. For networks of larger degree K these conditional boundaries erode due to the multiple paths along which the flow can equilibrate, as shown in Fig. 2(c). Nevertheless, the resilience boundary remains robust, being independent of d and occurring where $\alpha/\alpha_* \approx K/(K - 1)$ [27]. This can be understood by considering the ring network with common degree K when $n_s = 1$, $n_d = n - 1$, with initial flow apportioned equally across the K edges emanating from the single source. These edges are the most heavily loaded and so $\alpha_* \approx P^{\text{tot}}/K$. When one of these edges is removed to initiate a cascade, the flow is redistributed among the $K - 1$ remaining edges connected to the source and these must now supply flow to the rest of the network. Consequently, $\alpha_c \approx P^{\text{tot}}/(K - 1)$ and therefore $\alpha_c/\alpha_* \approx K/(K - 1)$. This relationship holds for larger networks, as shown in Fig. 2(d). The observed resilience boundary prompts defining a metric ρ to be

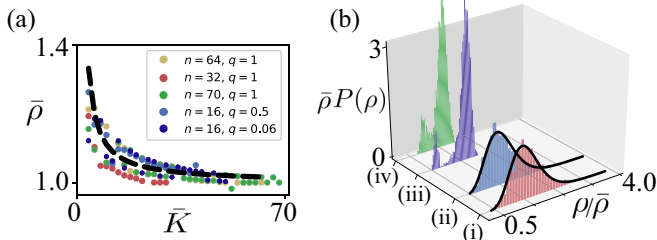$$\rho = \frac{\alpha_c}{\alpha_*} \equiv \frac{S^{-1}(1/2)}{\max(F_0)}, \tag{4}$$

FIG. 3. Variation of ρ in ensembles of 2000 random networks. (a) $\bar{\rho}(\bar{K})$ in Watts-Strogatz networks of size n and rewiring parameter q, with $n_s = 2$, $n_d = n - 2$. The dashed line is $\bar{K}/(\bar{K} - 1)$. (b) $P(\rho)$ in random networks with $(n_s, n_d, n_p) = (30, 30, 0)$. (i) $q = 0.1$ and (ii) $q = 0.6$. Both are fitted to lognormal(μ, σ^2) with $\mu = 1.18, 1.63$, and $\sigma = 0.25, 0.26$, respectively, and confirmed with Kolmogorov-Smirnov tests. (iii) and (iv) are for scale-free networks with $m_0 = 3$, $m = 4$, respectively.

which gauges the relative increase in edge capacity required to survive a cascade. The smaller the value of ρ, the more resilient is the network.

For ensembles of random networks ρ does not take a single value but rather is a random variable. The approximation for ρ when $n_s = 2$, $n_d = n - 2$ is replaced by $\bar{\rho} \approx \bar{K}/(\bar{K} - 1)$, where $\bar{K}$ is the mean degree that depends on n and q as shown in Fig. 3(a). For Watts-Strogatz networks the probability density $P(\rho)$ is log-normal with a mean value $\bar{\rho}$ that scales with network size n but with a similar standard deviation $\sigma \approx 0.255$ across the full range of rewiring parameters $q \in [0, 1]$ that encompass small-world to Poisson network topologies. This data collapse is illustrated in Fig. 3(b)(i,ii) for $q = 0.1, 0.6$, respectively; Fig. 3(b)(iii,iv) shows $P(\rho)$ for two scale-free networks that have a power-law degree distribution with initial node degrees $m_0 = 3, 4$, which are generated using the Albert-Barabasi preferential attachment method [28]. The range of ρ is smaller than that found for Watts-Strogatz networks, thereby indicating a greater resilience, and this agrees with earlier studies predicated on random edge removal [29,30]. When $n_s \approx n_d$ the distribution is bimodal, with the larger component of the distribution corresponding to when the edge initiating the cascade is connected to a hub. Networks grown by preferential attachment, such as social networks and the Internet, possess a scale-free structure, whereas electrical grids and road/rail transportation networks do not because their structures are often dictated by geographical constraints. This Rapid Communication is concerned chiefly with elec-

trical grids, so from here networks generated by the Watts-Strogatz procedure shall provide the structural substrate on which general results regarding resilience to failures can be deduced.

To explore the dependence of ρ on the composition of node types, note that the condition $n_s + n_d + n_p = n$ constrains the space of possible node configurations to a triangular simplex as illustrated in Fig. 4(a). The length of an edge of the simplex is the size n of the network and any point on the triangle represents a network with a unique node-type composition; the dot in the figure represents $(n_s, n_d, n_p) = (5, 10, 5)$. Selecting a network with given (q, K, n), and node types according to (n_s, n_d, n_p) that are located uniformly at random, the mean resilience $\bar{\rho}$ is calculated from 200 realizations and its value projected onto the corresponding location on the simplex.

Figure 4(b) shows $\bar{\rho}$ for regular lattices (i.e., $q = 0$) with $n = 100$, $K = 4$. The largest values of $\bar{\rho}$ and therefore the lowest resilience are located down two edges of the simplex, corresponding to networks with large numbers of sinks and very few sources, or vice versa. This means that the few source (or sink) nodes must generate (or absorb) the flow, and so incident edges must carry large flow volumes, making the network susceptible to failure. Resilient networks are spread throughout the interior region, which agrees with the intuition that a mix of node types has a high degree of redundancy and is therefore resilient because of the multiple flow paths such networks contain.

As q increases and the network structure becomes more random the morphology of $\bar{\rho}$ changes, the trend being shown in Figs. 4(c)–4(e). A band of greatest $\bar{\rho}$ broadens from the edges, moving into the interior region, until for $q \approx 0.12$ the largest values of $\bar{\rho}$ are found in the interior of the simplex. This represents an inversion in the resilience measure, counterintuitively showing that for networks in this regime of q a more heterogeneous mix of node types give less resilience than does a network with a few large suppliers of power. This behavior of $\bar{\rho}$ continues progressively until $q = 1$ (a Poisson network), where $\bar{\rho}$ has largest values in the center of the simplex and lowest values along two edges. In all cases the morphology of $\bar{\rho}$ is symmetric about the centerline, reflecting the reciprocity between sources and sinks.

The inversion in the behavior of $\bar{\rho}$ with q can be gauged by determining the value of $\Delta\rho = \bar{\rho}_{\text{left}} - \bar{\rho}_{\text{center}}$, where $\bar{\rho}_{\text{left}}$ and $\bar{\rho}_{\text{center}}$ are the values of $\bar{\rho}$ at the bottom left and center of the simplex, respectively. For regular lattices $\Delta\rho > 0$, whereas for Poisson networks $\Delta\rho < 0$. Figure 5(a) shows that for networks with $n = 60$, $\Delta\rho(q)$ decreases monotonically, the inversion occurring at the value of q where the network
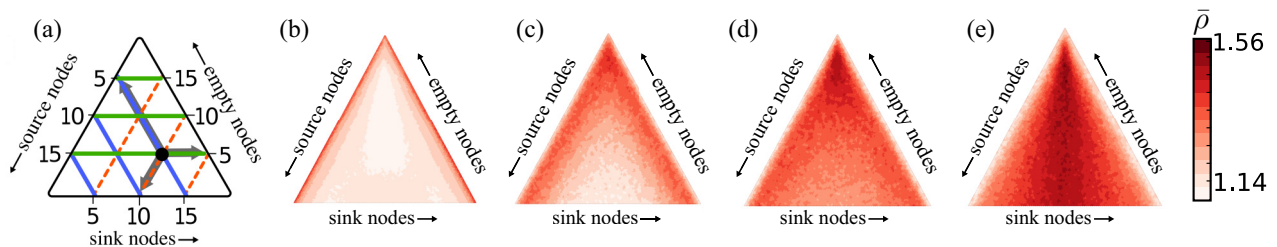

FIG. 4. (a) A sketch of the node configuration space simplex. The black dot represents a configuration of $(n_s, n_d, n_p) = (5, 10, 5)$. (b)–(e) $\bar{\rho}$ projected onto the simplex for networks of size $n = 100$, $K = 4$, and with $q = 0, 0.2, 0.4$, and 1, respectively.
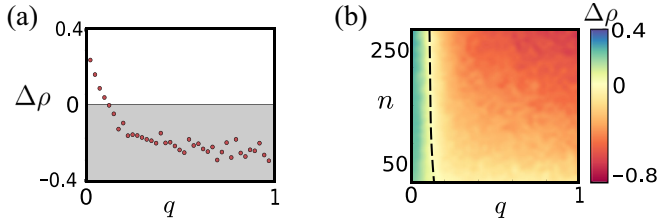
FIG. 5. (a) $\Delta\rho(q)$ for $n = 60$. (b) $\Delta\rho(q, n)$ where the dashed line is the locus of the inversion $\Delta\rho = 0$. All data points averaged over 200 realizations.
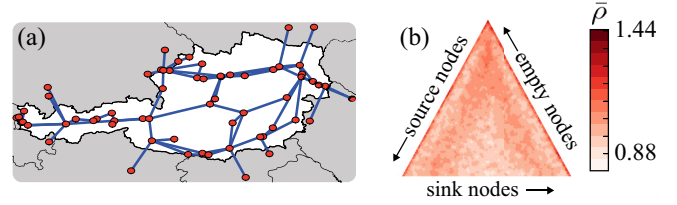

FIG. 6. (a) Power grid topology of Austria, constructed using data from Ref. [31]. (b) $\bar{\rho}$ for this grid projected onto the node configuration simplex. Each pixel is an ensemble average over 100 source-sink locations.

transitions from approximate order to the small-world regime. Figure 5(b) shows the dependence of $\Delta\rho$ with q and n; $\Delta\rho = 0$ is shown by the line and denotes the locus of the inversion, which is approximately independent of network size.

The preceding results consider homogeneous flow injection [i.e., $\zeta_v = 0$ in Eq. (3)] and edge capacity, reciprocal source-sink behavior, and cascades triggered by the removal of the most heavily loaded edge, which serve as a model for overloading failure. The impact of varying these model choices, and thus introducing several different types of heterogeneity, will now be considered. Cascades may be triggered by other unpredictable events such as lightning strikes or software failures and, moreover, generator output and consumer usage will vary. The behaviors and symmetry properties highlighted above persist if the cascade is initiated with a probability proportional to its initial load [27] and/or if the flow injection is perturbed by normally distributed noise with zero mean and the standard deviation selected to model generator variability, while still preserving node type in all realizations that we consider. These behaviors also persist for sources and sinks with gamma distributed strengths; see Ref. [27]. Unlike Refs. [8,10], this Rapid Communication has considered networks whose edge capacities are homogeneous. This choice is motivated by smaller-scale power networks that form our primary motivation, and whose dominant source of heterogeneity is node behavior rather than edge capacity. Nonetheless, the impact of edge capacity heterogeneity is investigated by perturbing α with Gaussian noise. These results, shown in Ref. [27], demonstrate that the features observed in the homogeneous case persist. However, for networks wherein source-sink reciprocity is broken, the morphology of the simplex plots is likewise no longer symmetric. This is illustrated in Ref. [27] for the case when only sink nodes have the ability to adjust their flow output to match supply and demand.

The resilience of the Austrian national grid is considered in Fig. 6(b). This network comprises $n = 67$, $m = 85$, and $\bar{K} = 2.53$, where each node represents a subnetwork of node

types and edges at both meso- and microscales that are unresolved by the data of Ref. [31]. Figure 6(b) shows $\bar{\rho}$ with each pixel entry averaged from 100 realizations of node-type location and with the sources and sinks assumed to have reciprocal strengths. The resilience landscape is characteristic of a state intermediate of those shown in Figs. 4(c) and 4(d) [27] includes two real-world examples of power grids which conform to the archetypes in Fig. 4.

This Rapid Communication has considered how the resilience of networks to cascading failures is affected by the composition of node types in addition to their topology. For the case of grids comprising a few large generators, Fig. 3(a) shows that the resilience can be approximated by $\bar{K}/(\bar{K} - 1)$, where $\bar{K} = \bar{K}(q, n)$. For the case of renewable energy electrical grids, the resilience is found using simplexes of the type shown in Fig. 4. Here, the appropriate node types correspond to locations of passivity, generation, or consumption of power, and these functions will mutate diurnally in response to changes in demand [24]. Crucially, although networks of a given topology with a homogenous node type composition can be resilient to failure, this is no longer the case for a network of the same topology but with a heterogeneous composition of node types. Regular lattices and ordered networks are most resilient when the number of node types are similar. This changes as the network's structure becomes increasingly disordered, with the least resilient configurations becoming those with similar numbers of node types. Despite this trend, there still exist regimes of resilience with a range of node-type compositions that can be accessed for highly randomized network structures.

[1] S. H. Strogatz, Nature (London) **410**, 268 (2001).

[2] R. Albert and A.-L. Barabási, Rev. Mod. Phys. **74**, 47 (2002).

[3] B. A. Carreras, V. E. Lynch, I. Dobson, and D. E. Newman, Chaos **12**, 985 (2002).

[4] X. Huang, I. Vodenska, S. Havlin, and H. E. Stanley, Sci. Rep. **3**, 1219 (2013).

[5] A. G. Haldane and R. M. May, Nature (London) **469**, 351 (2011).

[6] P. Crucitti, V. Latora, and M. Marchiori, Phys. Rev. E **69**, 045104(R) (2004).

[7] D. J. Watts, Proc. Natl. Acad. Sci. USA **99**, 5766 (2002).

[8] A. E. Motter and Y.-C. Lai, Phys. Rev. E **66**, 065102(R) (2002).

[9] Y.-C. Lai, A. E. Motter, and T. Nishikawa, *Complex Networks* (Springer, Berlin, 2004), pp. 299–310.

[10] A. E. Motter, Phys. Rev. Lett. **93**, 098701 (2004).

[11] D. Witthaut and M. Timme, Phys. Rev. E **92**, 032809 (2015).

[12] C. D. Brummitt, R. M. D'Souza, and E. A. Leicht, Proc. Natl. Acad. Sci. USA **109**, E680 (2012).

[13] S. Pahwa, C. Scoglio, and A. Scala, Sci. Rep. **4**, 3694 (2014).

[14] Y. Yang, T. Nishikawa, and A. E. Motter, Science **358**, eaan3184 (2017).

[15] Y. Yang and A. E. Motter, Phys. Rev. Lett. **119**, 248302 (2017).

[16] B. Schäfer, D. Witthaut, M. Timme, and V. Latora, Nat. Commun. **9**, 1975 (2018).

[17] M. Rohden, D. Jung, S. Tamrakar, and S. Kettemann, Phys. Rev. E **94**, 032209 (2016).

[18] Y. Zhang, A. Arenas, and O. Yağan, Phys. Rev. E **97**, 022307 (2018).

[19] S. Buldyrev, R. Parshani, G. Paul, H. Stanley, and S. Havlin, Nature (London) **464**, 1025 (2010).

[20] O. Smith, J. Crowe, R. O'Dea, and K. Hopcraft, Europhys. Lett. **127**, 18001 (2019).

[21] R. M. D'Souza, Science **358**, 860 (2017).

[22] A. Halu, A. Scala, A. Khiyami, and M. C. González, Sci. Adv. **2**, e1500700 (2016).

[23] D. E. Olivares, A. Mehrizi-Sani, A. H. Etemadi, C. A. Cañizares, R. Iravani, M. Kazerani, A. H. Hajimiragha, O. Gomis-Bellmunt, M. Saeedifard, R. Palma-Behnke, G. A. Jiménez-Estévez, and N. D. Hatziargyriou, IEEE Trans. Smart Grid **5**, 1905 (2014).

[24] S. Parhizi, H. Lotfi, A. Khodaei, and S. Bahramirad, IEEE Access **3**, 890 (2015).

[25] B. Stott, J. Jardim, and O. Alsac, IEEE Trans. Power Syst. **24**, 1290 (2009).

[26] D. J. Watts and S. H. Strogatz, Nature (London) **393**, 440 (1998).

[27] See Supplemental Material at http://link.aps.org/supplemental/10.1103/PhysRevE.101.020301 for analytic results and further data.

[28] A.-L. Barabasi and R. Albert, Science **286**, 509 (1999).

[29] D. S. Callaway, M. E. J. Newman, S. H. Strogatz, and D. J. Watts, Phys. Rev. Lett. **85**, 5468 (2000).

[30] R. Albert, H. Jeong, and A.-L. Barabási, Nature (London) **406**, 378 (2000).

[31] APG, https://www.apg.at/en/Stromnetz, accessed: 2019-05-17 .